

The warm interstellar medium around the Cygnus Loop*

Joaquín Bohigas^{1,3}, Jean Luc Sauvageot^{2,4} and Anne Decourchelle^{2,5}

*Based on observations collected at the Observatorio Astronómico Nacional, San Pedro Mártir, B.C., Mexico.

ABSTRACT

Observations of the oxygen lines [OII]3729 and [OIII]5007 in the medium immediately beyond the Cygnus Loop supernova remnant were carried out with the scanning Fabry-Pérot spectrophotometer ESOP. Both lines were detected in three different directions - east, northeast and southwest - and up to a distance of 15 pc from the shock front. The ionized medium is in the immediate vicinity of the remnant, as evinced by the smooth brightening of both lines as the adiabatic shock transition (defined by the X-ray perimeter) is crossed. These lines are usually brighter around the Cygnus Loop than in the general background in directions where the galactic latitude is $\geq 5^\circ$. There is also marginal (but significant) evidence that the degree of ionization is somewhat larger around the Cygnus Loop. We conclude that the energy necessary to ionize this large bubble of gas could have been supplied by an O8 or O9 type progenitor or the particles heated by the expanding shock front. The second possibility, though highly attractive, would have to be assessed by extensive modelling.

Subject headings: ISM: individual (Cygnus Loop) - supernova remnants - warm component

1. Introduction

An understanding of the properties and physics of the medium where supernova remnants (SNR's) expand is essential in order to develop consistent scenarios for their evolution and physical structure. In turn, the sequence of events leading to a supernova remnant and its demise define to a very large extent the structure, physical and chemical state and evolution of the interstellar medium. The Cygnus Loop is particularly well suited to study these questions. Being in an advanced evolutionary stage, different regions of the remnant are found interacting with different components of the interstellar medium. The remnant is close enough to study in great detail these interactions. In some circumstances the structure of the surrounding medium is deduced from observations of the SNR in different spectral domains (e.g. Graham *et al.* 1991; Hester, Raymond & Blair 1994; Decourchelle *et al.* 1997). When dealing with atomic or molecular gas this information has been gathered directly (e.g. DeNoyer 1975; Scoville *et al.* 1977).

¹Instituto de Astronomía, UNAM, Apdo. Postal 877, 22830 Ensenada, B.C., México

²C.E.A., DSM, DAPNIA, Service d'Astrophysique, C.E. Saclay, F91191, Gif sur Yvette Cedex, France

³Email address: jbb@bufadora.astrosen.unam.mx

⁴Email address: jsauvageot@cea.fr

⁵Email address: adecourchelle@cea.fr

Direct observations of ionized gas in the surrounding medium are considerably more complicated, since the emission lines arising from these regions are bound to be faint and prone to background confusion. In this respect the Cygnus Loop offers a substantial advantage, since it is placed at a large galactic latitude ($b = -8.6^\circ$).

Observations of faint emission lines in diffuse media have been carried out with a scanning Fabry-Pérot spectrophotometer. This technique has been successfully applied when searching for emission from Fe^{+9} and Fe^{+13} in SNR's (Ballet *et al.* 1989; Sauvageot *et al.* 1990; Sauvageot & Decouchelle 1995), or exploring line emission in the warm component of the interstellar medium (e.g. Reynolds 1983, 1985). In this paper we searched for line emission from warm ionized gas in the direction of the Cygnus Loop using such an instrument, ESOP (Dubreuil *et al.* 1995). In comparison with a grating instrument, ESOP can sample a large solid angle with a substantial luminosity advantage, at the cost of a reduced spectral range. It has no spatial resolution and is less efficient than direct imaging observations, but the line of interest can be isolated from other spectral features and the underlying continuum. This is a precious advantage when the line is faint.

A description of the instrumental setup and the process followed in data reduction is presented in §2. Results are described in detail in §3, and a discussion on the viability of several possible ionizing sources is given in §4. Finally, conclusions and research perspectives are summarized in §5.

2. Observations and data reduction

ESOP was mounted on the 1.5 meter telescope of the Observatorio Astronómico Nacional at San Pedro Mártir, B.C., México. Data was gathered in four runs: July 1994, October 1994, July 1995 and August 1996. The observations reported in this paper are for the [OII] lines at 3726 and 3729 Å, [OIII] at 5007 Å and HeI 5876 Å. We used narrow band (~ 15 Å FWHM) interference filters centered at these lines when $T = 20.5$ °C. Each observation consists of 50 to 100 scans of a hundred steps each. The integration time at each step is 170 ms. Thus, the typical total integration time for each data point is around 20 minutes. The free spectral range (FSR) was 11.3 Å during the first [OII] observations and 14.5 Å in the following ones, in both cases centered at 3727 Å (with the [O II] filter's FWHM = 15 Å). The FSR was not completely scanned by the Fabry-Pérot in the first [OII] observations. All [OIII] observations were conducted with a FSR of 10.8 Å centered at 5007 Å (with the [O III] filter's FWHM = 15 Å). Because our filters are well centered on the oxygen lines and the FSR is greater than half the filters' bandwidth, these are not contaminated. Sky lines lying far from the center of the filter, may have a contribution from another order. Since temperature variations shift the filter's transmission curve and humidity affects the air capacitance in the FP gap, the instrument works in a dry nitrogen atmosphere and is under temperature control (at $T \simeq 20.5$ °C, with $\delta T \simeq 0.2$ °C). White and comparison lamps were regularly measured in order to follow any bandpass drift in the filter or any variation in the FP gap. All observations were carried out with a 150" circular diaphragm.

Data reduction and analysis has been amply described in Ballet *et al.* (1989) and Sauvageot and Decouchelle (1995). It takes into account that the geocoronal contribution - lines and continuum - is unstable. No attempt is made to subtract a blank sky directly. Instead, the observation is modelled with a combination of sky and source lines and continuum. χ^2 tests are performed to estimate the statistical error of measurements.

Sky continuum and lines must be monitored carefully in this type of observations. Typical spectra at

the medium contiguous to the Cygnus Loop and randomly selected positions are presented in Figures 1 and 2 ([OII] and [OIII]).

Though absolute wavelength calibrations are wrong, relative ones (meaning dispersion) are correct. This is not consequential since this paper is only concerned with photometric results and there can hardly be any confusion regarding the identification of the line given its relative prominence (for instance, the bright feature at 5010.94 \AA in Figure 2b is obviously the [OIII]5007 line). For further clarity, arrows located on the upper part of Figures 1a, 1b, 2a and 2b indicate which is the line that is being studied. As can be seen, the O^+ lines are easily recognized and discriminated. Regarding the [OIII] filter, there can hardly be a confusion on the identification and measurement of [OIII]5007 since sky lines were found to be very weak in this spectral region. Since HeI 5876 was not detected outside the bright optical filaments of the Cygnus Loop, a discussion on the sky lines admitted by this filter is not necessary. Our observations were flux calibrated observing standard stars 29 Pisc and 58 Aql several times during the night. For the [OIII] calibration we had to take into account the contamination from the other order to the standard star continuum. At its worst, we estimate that the absolute values for the specific intensity are accurate at the 25% level, comparable to our statistical error bars.

3. Results

Regions within the Cygnus Loop and the medium surrounding it were observed in three directions (northeast, east and southwest), along lines approximately perpendicular to the shock front. Our observational pointings are shown in Figure 3. The shock front is defined as the outer X-ray boundary of the supernova remnant (Ku *et al.* 1984; Ballet & Rothenflug 1989). Our results for the O^+ and O^{+2} lines are compiled in Tables 1, 2 and 3 (NE, E and SW traces). The information contained in these tables is as follows: code name and coordinates for each position, angular distance (δ , in arcseconds) between the observed position and the shock front (negative values for regions inside the SNR), angular distance from the center of the SNR in terms of its radius, $1 + \delta/\theta$, where $\theta = 5850''$ is the angular radius of the Cygnus Loop (mean value of the semi-axes, Green 1988), the specific intensity of [OII]3729 \AA and [OIII]5007 \AA (henceforth [OII]3729 and [OIII]5007) in $10^{-7} \text{ erg cm}^{-2} \text{ s}^{-1} \text{ sr}^{-1}$, and the ratio of these lines (henceforth 3729/5007). Except for pointings in the optical filaments of the Cygnus Loop (such as NE0, NE1, E0, E1 and SW0), the ratio [OII]3727/3729 is always at the low density limit ($\simeq 0.67$, $N_e \leq 50 \text{ cm}^{-3}$), so there is no need to report the flux of the other [OII] line. Upper and lower bounds for the specific intensity are for a 90% confidence level in the fitting procedure. Uncertainties on the 3729/5007 line ratio were determined from these bounds. Both lines were detected at every position, some of them very far from the shock front: for instance, region E26 is $3894''$ distant from it, $\simeq 15 \text{ pc}$ at the distance where the Cygnus Loop is (770 pc). Except for the remnant's optical filaments, the HeI line was not detected.

The NE and E traces of [OII]3729 and [OIII]5007 as a function of $1 + \delta/\theta$ are plotted in Figure 4. As can be seen, both traces are nearly identical, and the specific intensities well away from the shock front are roughly constant (particularly [OII]3729). Notice that the adiabatic shock transition is revealed as [OII]3729 and [OIII]5007 brighten up smoothly as the X-ray perimeter of the SNR is crossed (at $1 + \delta/\theta = 1$). This brightening is caused by adiabatic compression of the plasma and enhanced line emissivities, which overcompensate the decreasing concentration of both ions since these are now immersed in a higher temperature medium. The SW trace is not plotted, but our measurements (see Table 4) also reveal the shock transition. The adiabatic transition is apparently complete at $1 + \delta/\theta \simeq 0.95$ or $\simeq 1 \text{ pc}$ inside the shock front. This is the most compelling evidence that this medium is not a projected HII region or parcel

from the general background, but is in the immediate vicinity of the Cygnus Loop. Our most distant pointing (region E26) is $\simeq 36$ pc away from the remnant’s center, which implies that the surrounding medium is ionized up to a distance of at least $\simeq 50$ pc. An additional and less conspicuous feature is that the specific intensity of both lines seems to rise slightly even before the shock front is crossed (from $1 + \delta/\theta \simeq 1.1$, or $\simeq 2$ pc away from the shock). This seems to indicate that the plasma immediately beyond the edge of the Cygnus Loop is being affected by the SNR before it encounters the blast wave, though this turn up may also be due to irregularities in the boundary of the remnant.

As mentioned above, [OII]3729 maintains an approximately constant level beyond $\simeq 0.1 - 0.2$ times the radius of the SNR. This level is nearly identical in the NE and E directions (for which we have sufficient data points). It is worth noticing that [OII]3729 is practically the same in regions separated by as much as $\simeq 5800''$ (NE22 and E26), some 22 pc at the distance to the Cygnus Loop. Thus, the [OII]3729 data indicates that the medium beyond the shock front of the Cygnus Loop is very extended, and quite possibly surrounds the eastern face of the remnant. Furthermore, the data for the SW trace, albeit limited, suggests that this medium exists all around the Cygnus Loop. [OIII]5007 does not display such a regular behaviour. Along the NE trace it dims slightly at positions NE8, NE9 and NE15, but it brightens up again further away (NE18 and NE22). Along the eastern trace [OIII]5007 behaves more regularly, weakening very noticeably in the two most distant pointings (E18 and E26). Thus, the [OIII]5007 observations imply that physical conditions in the surrounding medium are not homogeneous. If the temperature is uniform, there are variations in the oxygen degree of ionization: in the low density limit, $N(\text{O}^+)/N(\text{O}^{+2}) \simeq 2.7, 1.8$ or 1.5 in most positions, and up to $4.8, 3.3$ or 2.9 at E18 and E26 (for $T_e = 6000, 8000$ and 10000 °K). Alternatively, if the degree of ionization is constant, the temperature would have to be twice as large where [OIII]5007 is faintest. It seems difficult to maintain such high temperatures.

In order to assess if there is a difference between the medium surrounding the Cygnus Loop and the general background, observations were carried out on randomly selected directions located at $|b| \geq 5^\circ$, as the Cygnus Loop is. Specific intensities as low as $\sim 0.07 \times 10^{-7}$ erg cm $^{-2}$ s $^{-1}$ sr $^{-1}$ were measured, which gives an idea on the instrumental sensitivity. As expected, line brightness is not uniform in the galactic background. [OII]3729 was observed and detected 13 times over the four observing runs. Specific intensities comparable to some of those observed in regions contiguous to the Cygnus Loop (0.89 and 0.64×10^{-7} erg cm $^{-2}$ s $^{-1}$ sr $^{-1}$) were found in only two directions. Elsewhere they were markedly smaller, and in the mean [OII]3729 = $0.47 \pm 0.17 \times 10^{-7}$ erg cm $^{-2}$ s $^{-1}$ sr $^{-1}$. Out of 9 measurements, [OIII] was detected in 7 positions. [OIII]5007 = 0.68×10^{-7} erg cm $^{-2}$ s $^{-1}$ sr $^{-1}$ in the brightest sky background region, similar to what we found in some regions around the SNR, but in all other directions the line was much fainter. In the mean, [OIII]5007 = $0.25 \pm 0.24 \times 10^{-7}$ erg cm $^{-2}$ s $^{-1}$ sr $^{-1}$. In most sites we measured either one or the other line due to the complications involved in changing the instrumental setup. Both lines were measured only in two directions, where we found 3729/5007 = 3.13 and 7.80 . This implies that $N(\text{O}^+)/N(\text{O}^{+2}) \simeq 6.4$ and 16.8 (for $T_e = 8000$ °K), a rather low level of ionization. HeI 5876 was not detected, confirming the faintness of this line in the general background (Reynolds & Tufte 1995).

As far as we know, this is the first time that O $^+$ emission from the diffuse interstellar medium has been reported. Reynolds (1985) observed [OIII]5007 in three directions: the specific intensity was less than 0.5×10^{-7} erg cm $^{-2}$ s $^{-1}$ sr $^{-1}$ in one of them, 2 and 1.8×10^{-7} erg cm $^{-2}$ s $^{-1}$ sr $^{-1}$ in the other two. In these two, which are amongst the brightest sky background regions as defined by the H α intensity (Reynolds 1983), [OIII]5007 is substantially brighter than anything we find beyond the Cygnus Loop. We measured [OIII]5007 at the second brightest region ($l = 96.0^\circ, b = 0.0^\circ$) and obtained $0.68^{+0.20}_{-0.15} \times 10^{-7}$ erg cm $^{-2}$ s $^{-1}$ sr $^{-1}$, 2.6 times less than Reynolds. The discrepancy is probably related to the vast difference in aperture

sizes (49' *vs.* 2.5'), so that a region with particularly intense emission was included in Reynolds' diaphragm but not in ours.

Thus, there is a measurable background contribution to the intensity of the oxygen lines but, as can be seen from Tables 1 to 3, emission is generally larger in the medium surrounding the Cygnus Loop: [OII]3729 is at least 1.5 times brighter around the Cygnus Loop than in the general background, whereas [OIII]5007 is between 2 and 5 times more intense. Thus, the data supports the conclusion that [OII]3729 and [OIII]5007 in the medium just beyond the Cygnus Loop are usually brighter than in the general galactic background at least up to a distance of $\simeq 15$ pc from the shock front (about 0.6 times the radius of the remnant). There is also marginal but significant evidence indicating that the degree of ionization is higher in the medium around the Cygnus Loop.

The absence of HeI 5876 emission merits a discussion given the detection of [OIII]5007, which requires more energetic photons for this ion to exist (35.1 *vs.* 24.6 eV). We take notice that there is an antecedent: Reynolds (1985) found intense [OIII]5007 emission at $l = 194.0^\circ$ $b = 0.0^\circ$, but Reynolds & Tufte (1995) searched for HeI 5876 at this location with negative results, implying that $\text{He}^+/\text{He} \leq 0.3$. In general, $I(5876)/I(5007) = \epsilon(5876)/\epsilon(5007) \text{He}^+/\text{O}^{+2}$, where $\epsilon(5876)$ and $\epsilon(5007)$ are the emissivities for HeI 5876 and [OIII]5007. For cosmic abundances, and in the low density limit, $I(5876)/I(5007) = (0.08, 0.02, 0.008) (\text{He}^+/\text{He})(\text{O}/\text{O}^{+2})$ for $T = 6000, 8000$ and 10000 K. The fraction of doubly ionized oxygen is determined from the previously calculated O^+/O^{+2} ratio, assuming that there are no higher ionization stages and that $\text{O}^0/\text{O}^{+2} = 2$. And since $I(5007) \simeq 0.9 \times 10^{-7} \text{ erg cm}^{-2} \text{ s}^{-1} \text{ sr}^{-1}$ in the medium surrounding the Cygnus Loop, it follows that $I(5876) \simeq (0.42, 0.09, 0.03) (\text{He}^+/\text{He}) \times 10^{-7} \text{ erg cm}^{-2} \text{ s}^{-1} \text{ sr}^{-1}$. Finally, the non-detection of HeI 5876 implies that $I(5876) \leq 0.05 \times 10^{-7} \text{ erg cm}^{-2} \text{ s}^{-1} \text{ sr}^{-1}$ (our detection limit). Consequently, HeI 5876 emission will be under our detection threshold if $(\text{He}^+/\text{He}) \leq (0.17, 0.78 \text{ or } 1)$ for the aforementioned temperatures. Additionally, since He^+/He must be larger than O^{+2}/O , we conclude that the ambient temperature is larger than ~ 6000 K.

4. Discussion

The medium revealed by our observations has the general properties of the partially ionized warm component of the interstellar medium, which is so favourable for the observability of supernova remnants (Kafatos *et al.* 1980). But it is different insofar as it is generally brighter, and a couple of observations on sky background regions also suggest that the degree of ionization, given by $N(\text{O}^+)/N(\text{O}^{+2})$, is larger around the Cygnus Loop. On the other hand we did not detect HeI 5876 emission, and in this respect there is no difference between the medium just beyond the Cygnus Loop and the general galactic background (Reynolds and Tufte 1995). But there are several reasons to expect somewhat different properties in the medium surrounding the Cygnus Loop: the remnant has been included in the so called Cygnus superbubble, along with several OB associations, the SN progenitor might have been a source of ionizing energy, the SN itself produced a large amount of UV photons and, finally, ionizing radiation is also generated by the expanding shock wave. We will discuss these possible sources in the following paragraphs.

The Cygnus Loop is at the southern edge of the extremely rich and complex region known as the Cygnus superbubble, which has been extensively described and analysed by Bochkarev & Sitnik (1985). The superbubble has seven OB associations containing 48 O type stars and nearly 70 B type stars. With the exception of Cyg OB4 and Cyg OB7, all of them are at a distance of 1.2 kpc or more. Cyg OB7 is at approximately the same distance as the Cygnus Loop, but is located some 20° away from it (about 280

pc). Cyg OB4 is also relatively near, but though it has been classified as an OB association, it does not contain any O or B star. Thus, it is doubtful that these OB associations can account for the ionization of the medium surrounding the Cygnus Loop. We also contemplated the possibility that this medium is an extended low surface brightness HII region produced by an early type star in the vicinity of the SNR. A visual inspection of POSS plates and a thorough search of O and B stars catalogs (Cruz-González *et al.* 1974; Garmany, Conti & Chiosi 1982) renders no support to this possibility. The SAO catalog was also explored with negative results.

The ionized medium around the Cygnus Loop may also be the relic HII region of the progenitor star. The progenitor should have produced $P_{UV} \sim 5 \times 10^{48} N_H^2$ UV photons per second to create a 50 pc Strömgren sphere if the medium is fully ionized, as the presence of O^{+2} seems to imply (but notice that Graham *et al.* (1991) found shocked H_2 in the Cygnus Loop). The mean particle density in the medium where the remnant evolved at least until recently is $\sim 0.1 - 0.2 \text{ cm}^{-3}$ (Ku *et al.* 1984; Levenson *et al.* 1997), which signifies that the required spectral type of the progenitor star must have been earlier than or equal to B0. Furthermore, the 3729/5007 ratio ($\simeq 1$ with no reddening correction, about 1.5 for a 1 magnitude visual extinction), implies that the effective temperature of the ionizing star is close to 35000 K (Stasinska 1978), corresponding to a spectral type slightly later than O8. Under this hypothesis, the mass of the progenitor would have been between 20 and 25 M_\odot . Such a star spends most of its lifetime as a blue giant and only $\sim 1\%$ of its existence ($\sim 10^5$ yr) as a red supergiant (Brunish & Truran 1982). This is substantially less than the recombination time ($\sim 10^5/N_H$ yr). Thus, an O8 or O9 progenitor surrounded by a pervasive low density medium can account for our observations.

On the other hand, based on the X-ray morphology of the SNR, Levenson *et al.* (1997) favor a scenario with a progenitor of spectral type later than B0. According to them, the Cygnus Loop evolved within the ~ 20 pc homogeneous low-density HII region created by this progenitor, and is now bursting into the relatively dense and inhomogeneous medium surrounding it, in the manner described by McKee *et al.* (1984). This would explain the existence of abundant local inhomogeneities on the external surface of a nearly circular remnant. Notice that an earlier type progenitor would create a larger homogeneous cavity.

The UV radiation produced by the SN explosion can also be an important ionizing source, as was palpably revealed when narrow emission lines appeared in the UV spectra of SN1987A ~ 70 days after the event (Fransson *et al.* 1989). At least some 10^{44} erg of ionizing energy was required to produce these lines (Fransson *et al.* 1989), substantially less than the $10^{46} - 10^{47}$ erg that hydrodynamical models had predicted for the ionizing burst of SN1987A (Shigeyama, Nomoto & Hashimoto 1988; Woosley 1988). But values as large as $10^{48} - 10^{49}$ erg in ionizing energy have been mentioned in the literature (Chevalier 1977; Chevalier 1990). If the mean photon energy is 20 eV, the largest radiation “pulse” ionizes the surrounding medium up to a distance of $14 N_H^{-1/3}$ pc at the most, where N_H is the mean hydrogen density. The density would have to be smaller than 0.02 cm^{-3} in order to produce a 50 pc bubble of ionized gas. Observations and models for the evolution of the Cygnus Loop lead to substantially larger mean densities in the surrounding medium (e.g. Ku *et al.* 1984).

Ultraviolet photons are constantly being supplied by the expansion of the SNR as the shock heated particles produce ionizing radiation as they move downstream. This has been discussed in the numerous radiative shock wave models developed over the last 25 years (e.g. Cox 1972; Dopita 1977; Raymond 1979; Cox & Raymond 1985; Shull & McKee 1979; Binette, Dopita & Tuohy 1985; Sutherland, Bicknell & Dopita 1993). The effect of this ionizing radiation on the upstream gas has been considered in the context of AGN (Daltabuit & Cox 1972) or, more recently, the emission line filaments in Centaurus A (Sutherland *et al.* 1993). A review on the many topics opened to this question was written by Dopita (1995). But to the

best of our knowledge, little attention has been directed to the effect of the photoionizing flux of SNR's on the galactic interstellar medium. At this point we are specifically interested in determining the size of the bubble of ionized gas that can result from the UV flux produced by the shock heated particles, in order to establish if this energy source is sufficient to create the large sphere of ionized gas that is implied by our observations. An estimate of this quantity can be determined following a very simple line of arguments. The number of upstream moving photons produced each second by a SNR expanding into a medium with density N_0 , is given by

$$P_{UV} = 4\pi R_0^2 N_0 V_0 \phi_{UV} \quad (1)$$

where ϕ_{UV} is the number of upstream moving UV photons produced per shocked particle, and R_0 and V_0 are the remnant's radius and velocity. If this quantity is equal to the number of recombinations, then

$$(R_i/R_0)^3 = 74.8 V_7 \phi_{UV} / (N_0 R_{pc}) + 1 \quad (2)$$

where R_i is the radius of the ionized volume measured from the remnant's center, V_7 is the shock velocity in 100 km s^{-1} and R_{pc} is the radius of the SNR in parsec. The latter can be determined assuming that the evolution of the Cygnus Loop is described by Sedov's (1959) solution. In the case of the Cygnus Loop this assumption can be objectionable, but is probably adequate given the scope of this discussion. In this case,

$$R_{pc} = 19.4 (E_{50}/N_0)^{1/3} V_7^{-2/3} \quad (3)$$

where E_{50} is the kinetic energy deposited in the SNR in 10^{50} erg. Equations (2) and (3) lead to,

$$(R_i/R_0)^3 = 3.86 V_7^{5/3} \phi_{UV} / (E_{50} N_0^2)^{1/3} + 1 \quad (4)$$

For a given metallicity the number of ionizing photons per particle only depends on the shock velocity. Shull & McKee (1979) present their results in a more amenable fashion than Binette *et al.* (1985) and Dopita (1995), and the following analytical approximation for ϕ_{UV} can be derived from their work,

$$\phi_{UV} \simeq 1.08 (V_7^2 - 0.58) \quad (5)$$

Their calculations stop at $V_7 = 1.3$, but it is probably correct to extend this approximation to larger velocities (the functional dependence should not change, see Dopita 1995). For an equilibrium cooling function the shock can be radiative up to $V_7 \simeq 1.5 - 2$. But the plasma behind the shock front will be underionized with respect to collisional ionization equilibrium, and in this condition cooling is more efficient (Sutherland and Dopita 1993). Thus, the shock will become radiative at somewhat higher velocities.

The size of the region that can be ionized by photons produced by the shock heated particles, R_i , can now be determined from equations (3), (4) and (5). Results as a function of shock velocity are presented in Table 4 for various combinations of (E_{50}, N_0) : (1,1), (3,0.2) and (1,0.2). The second set of parameters is representative of the Cygnus Loop (Ku *et al.* 1984). As can be seen, a 50 pc ionized bubble can be produced even in the most conservative case. The size of the region of ionized gas is surprisingly large when the

standard parameters for the Cygnus Loop are considered. Furthermore, since the evolutionary timescale of a SNR is much shorter than the recombination time, it follows that the ionizing radiation supplied by the remnant as it continues evolving would further increase the size of the ionized region. Consequently it appears that, at least from the point of view of the energy budget, radiative shock waves can produce a very extended environment of ionized matter around them. A stricter analysis is no doubt necessary, but it seems improbable that it will lead to a qualitatively different conclusion on the number of ionizing photons produced by the expanding SNR, and consequently on the size of the region that will be influenced by them. But if there seems to be little doubt that SNR's can ionize large regions of the interstellar medium, it has to be shown that these objects can do so in the course of their evolution. This is an essential point in relation to this work.

It is worth pointing out that, in comparison to other ionizing sources, the ionizing energy produced by SNR's can be of considerable importance. Integrating equation (1) with the aforementioned hypotheses, it is easy to see that a SNR will produce $1.2 \times 10^{60} E_{50}$ UV photons as it slows down from 250 to 80 km s⁻¹, $\sim 30\%$ of its initial kinetic energy if the mean photon energy is 15 eV. On the other hand, any main sequence B0 or O type star will produce some 10^{63} UV photons during its lifetime. Considering that SNR's are some 20 times more abundant than O type stars, this implies that, during their radiative phase, SNR's will generate about a tenth of the UV flux produced by all B0 and O type stars. This is not a small number. Furthermore, SNR's will be a major source of UV radiation in stellar systems lacking massive stars.

5. Conclusions

Evidence was presented for the existence of an extended ionized medium surrounding the eastern face of the Cygnus Loop, and quite possibly the entire remnant. The shock transition is revealed by the slow rise in the specific intensity of [OII]3729 and [OIII]5007 as the X-ray perimeter of the SNR is crossed. This is indisputable proof that this medium is in the immediate vicinity of the Cygnus Loop. Our most distant pointing (region E26) is $\simeq 36$ pc away from the remnant's center, which implies that there is ionized gas at least up to a distance of $\simeq 50$ pc. It would be interesting to observe more distant regions, preferably in the O⁺² line, in order to see whether there is an outer boundary or the medium merges smoothly with the general background. The medium around the Cygnus Loop is somewhat different to the general galactic background: [OII]3729 and [OIII]5007 are usually brighter, and there are indications that the degree of ionization, given by $N(\text{O}^+)/N(\text{O}^{+2})$, is also larger around the SNR. On the other hand it is similar insofar as HeI 5876 emission is also conspicuously absent.

We explored several possible sources which may produce the ionizing energy required to account for the existence of this medium. Viable external sources, such as an isolated early type star or an OB association, could not be found. We also concluded that the ionizing radiation produced by the SN explosion was probably insufficient. An early type (between O8 and O9, but closer to the former) progenitor embedded in a low density medium can account for the required energy budget, but a later type progenitor has been suggested by Levenson *et al.* (1997). Finally, we showed that the UV radiation produced by the shock heated particles *can* generate a large bubble of ionized gas, but detailed modelling is required in order to see if it *will* do so during the SNR's lifetime.

From the observational point of view, it is advisable to inspect other emission lines in order to explore the spectral properties of the medium surrounding the Cygnus Loop, and decide if it is indeed distinct to the warm component of the interstellar medium. Unfortunately, our instrumental resolution is insufficient

to discriminate coronal and galactic $H\alpha$ emission, the key line in Reynolds' research on the properties of this component of the interstellar medium. But other spectral lines, such as [NII]6584 Å and [SII]6717,6731 Å, are open to inspection since they are less affected by geocoronal emission. Needless to say, similar observations of the medium surrounding other SNR's should furnish valuable information. Targets located away from the galactic plane are preferable, since background confusion is avoided. Further research along these lines may be helpful regarding the still open question on the origin of the warm partially ionized component of the interstellar medium, given the relatively large flux of UV photons produced by radiative shock waves. As we pointed out, the photoionizing flux produced by SNR's will be particularly important in systems lacking massive stars.

Acknowledgments The excellent support received from C. Blondel, P. Mulet and the technical staff at San Pedro Mártir observatory is gratefully acknowledged. We thank the anonymous referee for the comments and suggestions that lead to great improvements on this paper, and in particular for pointing out the effect of contamination from the other order to the standard star continuum.

References

- Ballet, J., Caplan, J., Rothenflug, R., Dubreuil, D. & Soutoul, A. 1989, *A&A* 211, 217
- Ballet, J. & Rothenflug, R. 1989, *A&A* 218, 277
- Binette, L., Dopita, M.A. & Tuohy, I.R. 1985, *ApJ* 297, 476
- Bochkarev, N.G. & Sitnik, T.G. 1985, *Ap&SS* 108, 237
- Brunish, W.M. & Truran, J.W. 1982, *ApJS* 49, 447
- Chevalier, R.A. 1977, *ARA&A* 15, 175
- Chevalier, R.A. 1990, in *Supernovae*, *A&A Library*, ed. A.G. Petschek (Springer-Verlag, New York), 91
- Cox, D.P. 1972, *ApJ* 178, 143
- Cox, D.P. & Raymond, J.C. 1985, *ApJ* 298, 651
- Cruz-Gonzalez, C., Recillas-Cruz, E., Costero, R., Peimbert, M. & Torres-Peimbert, S. 1974, *RevMexAA* 1, 211
- Daltabuit, E. & Cox, D.P. 1972, *ApJ* 173, L173
- Decourchelle, A., Sauvageot, J.L., Ballet, J. & Aschenbach, B. 1997, *A&A* 326, 811
- DeNoyer, L.K. 1975, *ApJ* 196, 479
- Dopita, M.A. 1977, *ApJS* 33, 437
- Dopita, M.A. 1995, in *The analysis of emission lines*, *STScI Symp. Series 8*, ed. R.E. Williams & M. Livio (Cambridge, New York), 65
- Dubreuil, D., Sauvageot, J.L., Blondel, C., Dhenain, G., Mestreau, P. & Mullet, P. 1995, *Exp. Astron.* 6, 257

- Fransson, C., Cassatella, A., Gilmozzi, R., Kirshner, R.P., Panagia, N., Sonneborn, G. & Wamsteker, W. 1989, *ApJ* 336, 429
- Garmany, C.D., Conti, P.S., Chiosi, C. 1982, *ApJ* 263, 777
- Georgelin, Y.M., Lortet-Zuckerman, M.C. & Monnet, G. 1975, *A&A* 42, 273
- Graham, J.R., Wright, G.S., Hester, J.J. & Longmore, A.J. 1991, *AJ* 101, 175
- Green, D. A. 1988, *Ap&SS* 148, 3
- Hester, J.J., Raymond, J.C. & Blair, W.P. 1994 *ApJ* 1994., *ApJ* 420, 721
- Kafatos, M., Sofia, S., Bruhweiler, F. & Gull, T. 1980, *ApJ* 242, 294
- Ku, W.H.M., Kahn, S.M., Pisarski, R. & Long, K.S. 1984, *ApJ* 278, 615
- Levenson, N.A., Graham, J.R., Aschenbach, W.P., Blair, W.P., Brinkmann, W., Busser, J.U., Egger, R., Fesen, R.A., Hester, J.J., Kahn, S.M., Klein, R.M., McKee, C.F., Petre, R., Pisarski, R., Raymond, J.C. & Snowden, S.L. 1997, *ApJ* 484, 304
- McKee, C.F., Van Buren, D. & Lazareff, B. 1984, *ApJ* 278, L115
- Raymond, J.C. 1979, *ApJS* 35, 419
- Reynolds, R.J. 1983, *ApJ* 268, 698
- Reynolds, R.J. 1985, *ApJ* 298, L27
- Reynolds, R.J. & Tuftte, S.L. 1995, *ApJ* 439, L17
- Sauvageot, J.L. & Decourchelle, A. 1995, *A&A* 296, 201
- Sauvageot, J.L., Ballet, J., Dubreuil, D., Rothenflug, R., Soutoul, A. & Caplan, J. 1990, *A&A* 232, 203
- Scoville, N.Z., Irvine, W.M., Wannier, P.G. & Predmore, C.R. 1977, *ApJ* 216, 320
- Sedov, L.I. 1959, *Similarity and dimensional methods in mechanics*, Academic Press, New York.
- Shigeyama, T., Nomoto, K. & Hashimoto, M. 1988, *A&A* 196, 141
- Shull, J.M. & McKee, C.F. 1979, *ApJ* 227, 131
- Stasinska, G. 1978 *A&AS* 32, 429
- Sutherland, R.S. & Dopita, M.A. 1993, *ApJS* 88, 253
- Sutherland, R.S., Bicknell, G.V. & Dopita, M.A. 1993, *ApJ* 414, 510
- Woosley, S.E. 1988, *ApJ* 324, 466

Figure Captions

Figure 1. [OII] lines: (a) sky, (b) region NE14.

Figure 2. [OIII] lines: (a) sky, (b) region NE18.

Figure 3. Observational pointings: (a) NE, (b) E and (c) SW. North is up, east is to the left.

Figure 4. [OII] and [OIII] NE and E traces.

Table 1. Northeastern trace

	RA (1950)	DEC	$\delta(^{\circ})$	$1 + \delta/\theta$	I([OII]3729)	I([OIII]5007)	3729/5007
NE0	20 53 55.8	+31 35 05	-884	0.85		30.1 ^{+6.1} _{-6.1}	
NE1	20 54 05.0	+31 37 35	-663	0.89	79.0 ^{+0.0} _{-0.0}	67.8 ^{+9.3} _{-9.3}	1.17 ^{+0.18} _{-0.14}
NE2	20 54 20.0	+31 39 20	-390	0.93	2.91 ^{+0.23} _{-0.34}	2.89 ^{+0.21} _{-0.60}	1.01 ^{+0.37} _{-0.18}
NE3	20 54 19.0	+31 41 05	-325	0.94	1.71 ^{+0.19} _{-0.23}	1.83 ^{+0.36} _{-0.31}	0.93 ^{+0.32} _{-0.26}
NE4	20 54 26.0	+31 42 50	-162	0.97	1.13 ^{+0.16} _{-0.22}	1.38 ^{+0.33} _{-0.33}	0.82 ^{+0.41} _{-0.30}
NE5	20 54 33.0	+31 44 35	0	1	1.02 ^{+0.18} _{-0.23}	0.85 ^{+0.24} _{-0.24}	1.20 ^{+0.76} _{-0.47}
NE6	20 54 40.0	+31 46 20	162	1.03	0.90 ^{+0.20} _{-0.10}	0.99 ^{+0.48} _{-0.35}	0.91 ^{+0.82} _{-0.37}
NE7	20 54 47.0	+31 48 05	325	1.06	0.80 ^{+0.15} _{-0.21}	0.96 ^{+0.24} _{-0.25}	0.83 ^{+0.50} _{-0.34}
NE8	20 54 54.0	+31 49 50	487	1.08	0.67 ^{+0.13} _{-0.19}	0.71 ^{+0.15} _{-0.19}	0.94 ^{+0.58} _{-0.38}
NE9	20 55 01.0	+31 51 35	650	1.11	0.78 ^{+0.29} _{-0.23}	0.73 ^{+0.26} _{-0.21}	1.07 ^{+1.02} _{-0.42}
NE12	20 55 22.0	+31 54 50	1137	1.19	0.65 ^{+0.10} _{-0.21}		
NE14	20 55 31.0	+32 00 00	1485	1.25	0.70 ^{+0.10} _{-0.21}		
NE15	20 55 43.0	+32 02 05	1702	1.29	0.77 ^{+0.20} _{-0.25}	0.65 ^{+0.19} _{-0.16}	1.18 ^{+0.88} _{-0.56}
NE18	20 56 04.0	+32 07 20	2189	1.37	0.83 ^{+0.13} _{-0.18}	0.85 ^{+0.31} _{-0.31}	0.98 ^{+0.81} _{-0.42}
NE22	20 56 23.0	+32 17 02	2754	1.47	0.65 ^{+0.20} _{-0.15}	0.95 ^{+0.30} _{-0.24}	0.69 ^{+0.33} _{-0.37}

Intensity in $10^{-7} \text{erg cm}^{-2} \text{s}^{-1} \text{sr}^{-1}$

Table 2. Eastern trace

	RA (1950) DEC	$\delta(^{\circ})$	$1+ \delta/\theta$	I([OII]3729)	I([OIII]5007)	3729/5007
E0	20 55 13.8 +30 54 30	-705	0.88	45.20 $^{+1.30}_{-1.70}$	198.0 $^{+15.8}_{-15.8}$	0.23 $^{+0.02}_{-0.03}$
E1	20 55 24.0 +30 54 30	-531	0.91	18.20 $^{+0.40}_{-1.10}$	111.3 $^{+11.8}_{-11.8}$	0.16 $^{+0.02}_{-0.02}$
E2	20 55 34.0 +30 54 30	-354	0.94	2.98 $^{+0.36}_{-0.27}$	4.86 $^{+0.24}_{-0.25}$	0.62 $^{+0.10}_{-0.09}$
E3	20 55 44.0 +30 54 30	-177	0.97	1.45 $^{+0.03}_{-0.20}$	2.04 $^{+0.34}_{-0.70}$	0.71 $^{+0.39}_{-0.18}$
E4	20 55 54.0 +30 54 30	0	1.	1.54 $^{+0.10}_{-0.35}$	1.43 $^{+0.29}_{-0.25}$	1.08 $^{+0.31}_{-0.38}$
E5	20 56 04.0 +30 54 30	177	1.03	1.56 $^{+0.14}_{-0.47}$	1.61 $^{+0.43}_{-0.35}$	0.96 $^{+0.38}_{-0.42}$
E6	20 56 14.0 +30 54 30	354	1.06	1.15 $^{+0.22}_{-0.29}$	2.14 $^{+0.34}_{-0.24}$	0.54 $^{+0.18}_{-0.19}$
E8	20 56 34.0 +30 54 30	708	1.12	0.91 $^{+0.16}_{-0.19}$	1.09 $^{+0.26}_{-0.33}$	0.84 $^{+0.56}_{-0.30}$
E10	20 56 54.0 +30 54 30	1062	1.18	0.78 $^{+0.15}_{-0.24}$	1.04 $^{+0.18}_{-0.39}$	0.75 $^{+0.68}_{-0.30}$
E14	20 57 34.0 +30 54 30	1770	1.30	0.77 $^{+0.11}_{-0.14}$	0.93 $^{+0.23}_{-0.21}$	0.83 $^{+0.40}_{-0.29}$
E18	20 58 14.0 +30 54 30	2478	1.42	0.81 $^{+0.10}_{-0.19}$	0.45 $^{+0.18}_{-0.16}$	1.80 $^{+1.37}_{-0.81}$
E26	20 59 34.0 +30 54 30	3894	1.67	0.61 $^{+0.16}_{-0.08}$	0.46 $^{+0.20}_{-0.15}$	1.31 $^{+1.15}_{-0.29}$

Intensity in $10^{-7} \text{erg cm}^{-2} \text{s}^{-1} \text{sr}^{-1}$

Table 3. Southwestern trace

	RA (1950) DEC	$\delta(^{\circ})$	$1+ \delta/\theta$	I([OII]3729)	I([OIII]5007)	3729/5007
SW0	20 44 55.3 +30 00 36	-631	.89	7.02 $^{+0.48}_{-0.52}$	15.1 $^{+0.9}_{-0.8}$	0.46 $^{+0.06}_{-0.06}$
SW1	20 44 35.3 +29 57 36	-314	0.95		48.5	
SW1.5	20 44 25.3 +29 56 08	-158	0.97	1.71 $^{+0.16}_{-0.20}$	1.66 $^{+0.35}_{-0.64}$	1.03 $^{+0.79}_{-0.28}$
SW2	20 44 15.3 +29 54 36	0	1	1.14 $^{+0.22}_{-0.17}$	0.78 $^{+0.54}_{-0.30}$	1.47 $^{+1.38}_{-0.74}$
SW4	20 43 35.3 +29 48 36	633	1.11	0.85 $^{+0.23}_{-0.18}$	0.89 $^{+0.16}_{-0.34}$	0.96 0.32 1.00

Intensity in $10^{-7} \text{erg cm}^{-2} \text{s}^{-1} \text{sr}^{-1}$

Table 4. Photoionizing shock

V_7	$E_{50} = 1,$ R_{pc}	$N_0 = 1$ R_i (pc)	$E_{50} = 3,$ R_{pc}	$N_0 = 0.2$ R_i (pc)	$E_{50} = 1,$ R_{pc}	$N_0 = 0.2$ R_i (pc)
1.0	19	27	48	79	33	61
1.5	15	36	37	112	25	87
2.0	12	44	30	136	21	107
2.5	11	50	26	157	18	123

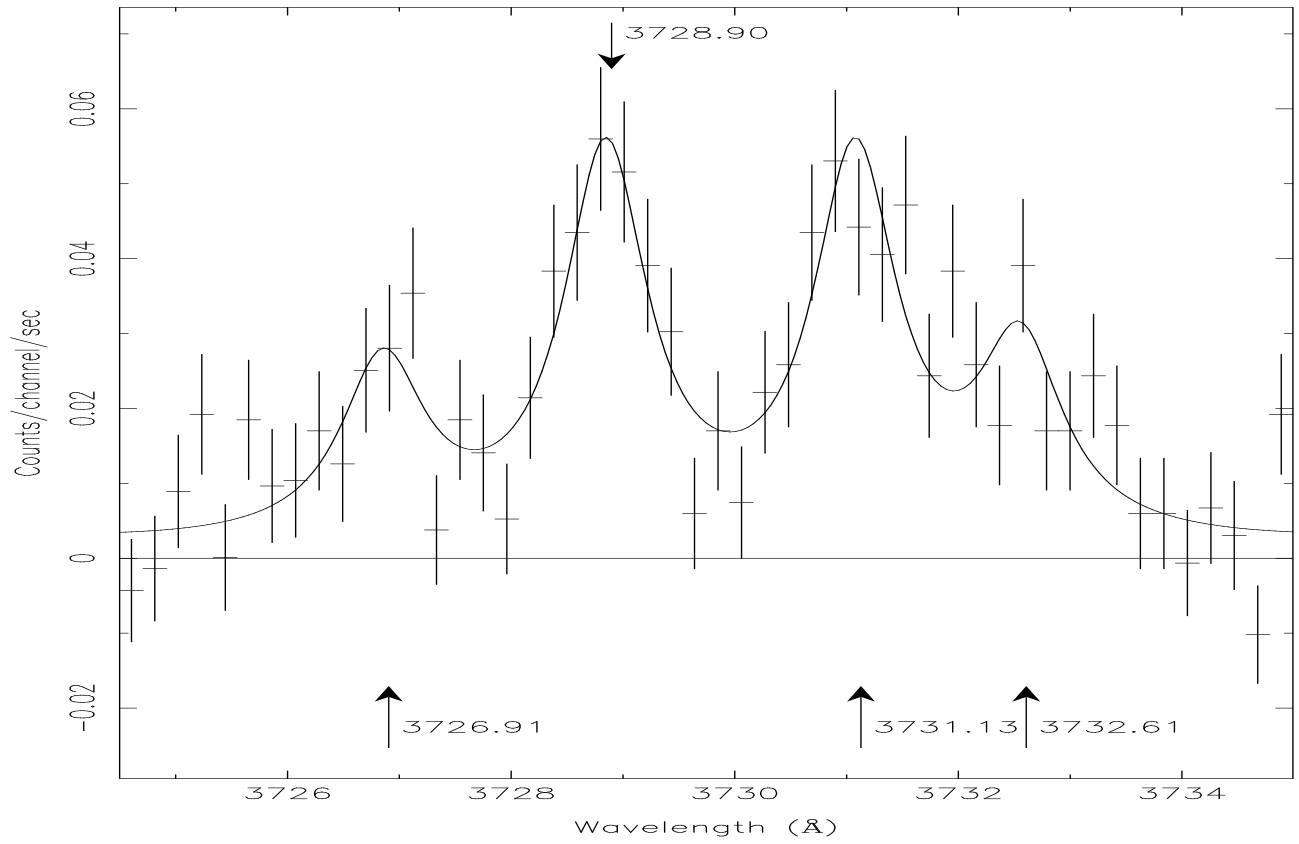


Figure 1a.

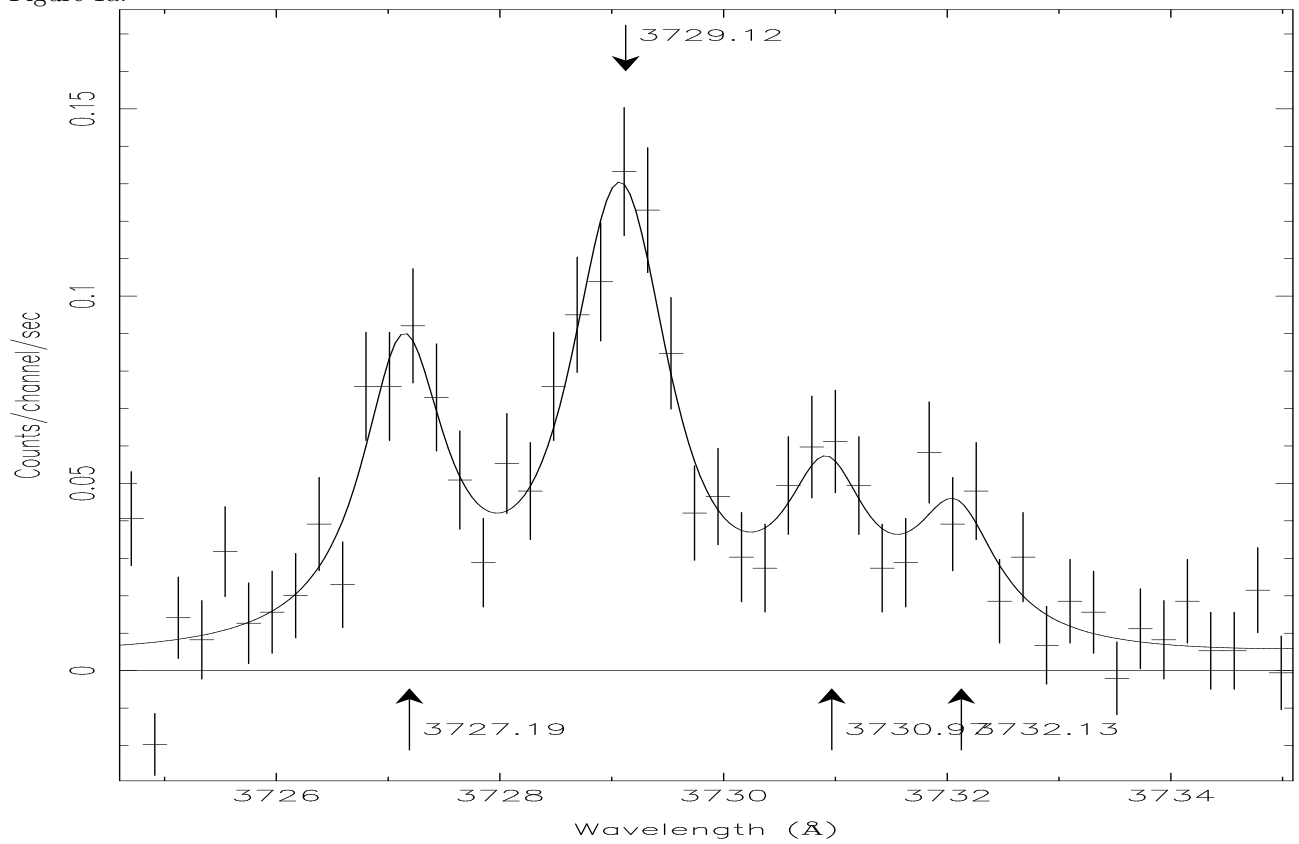


Figure 1b.

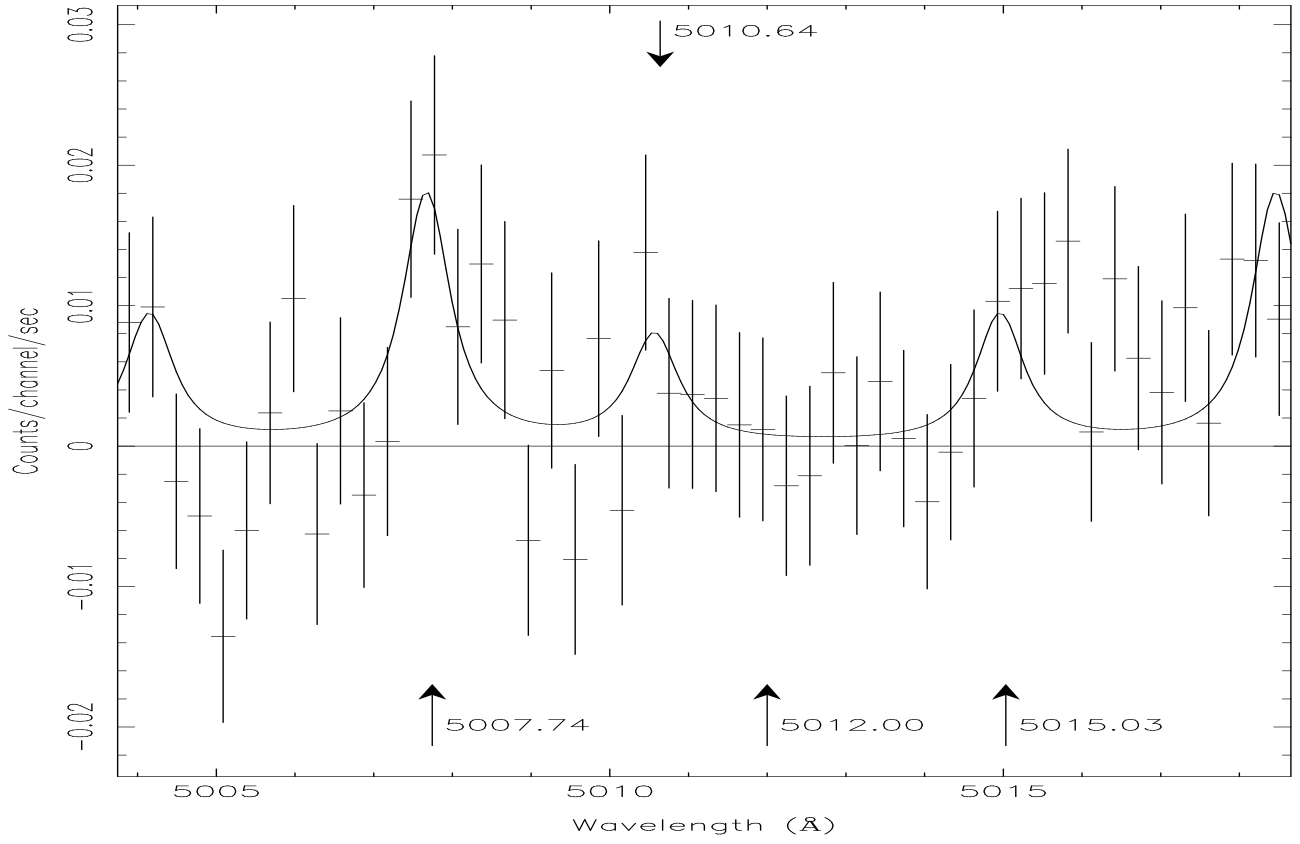


Figure 2a.

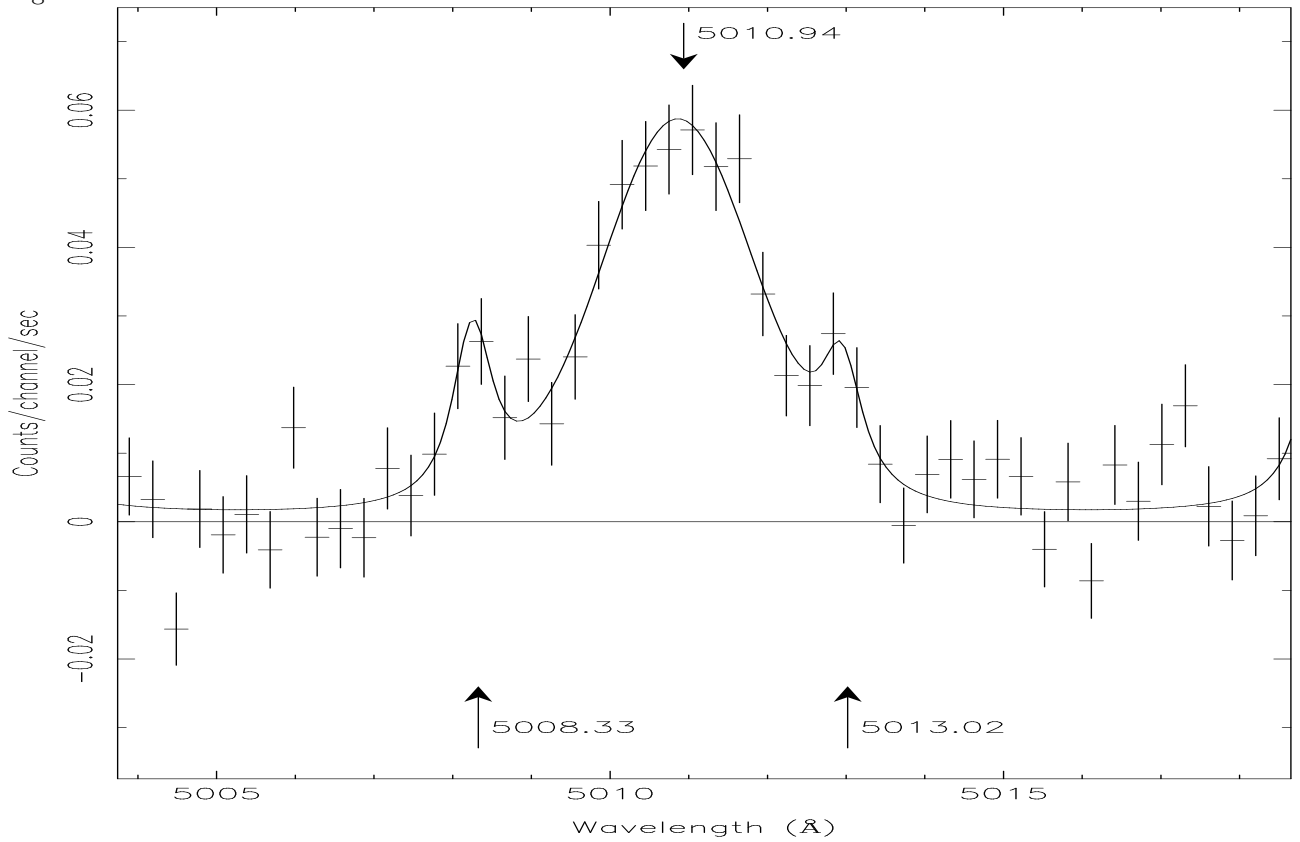


Figure 2b.

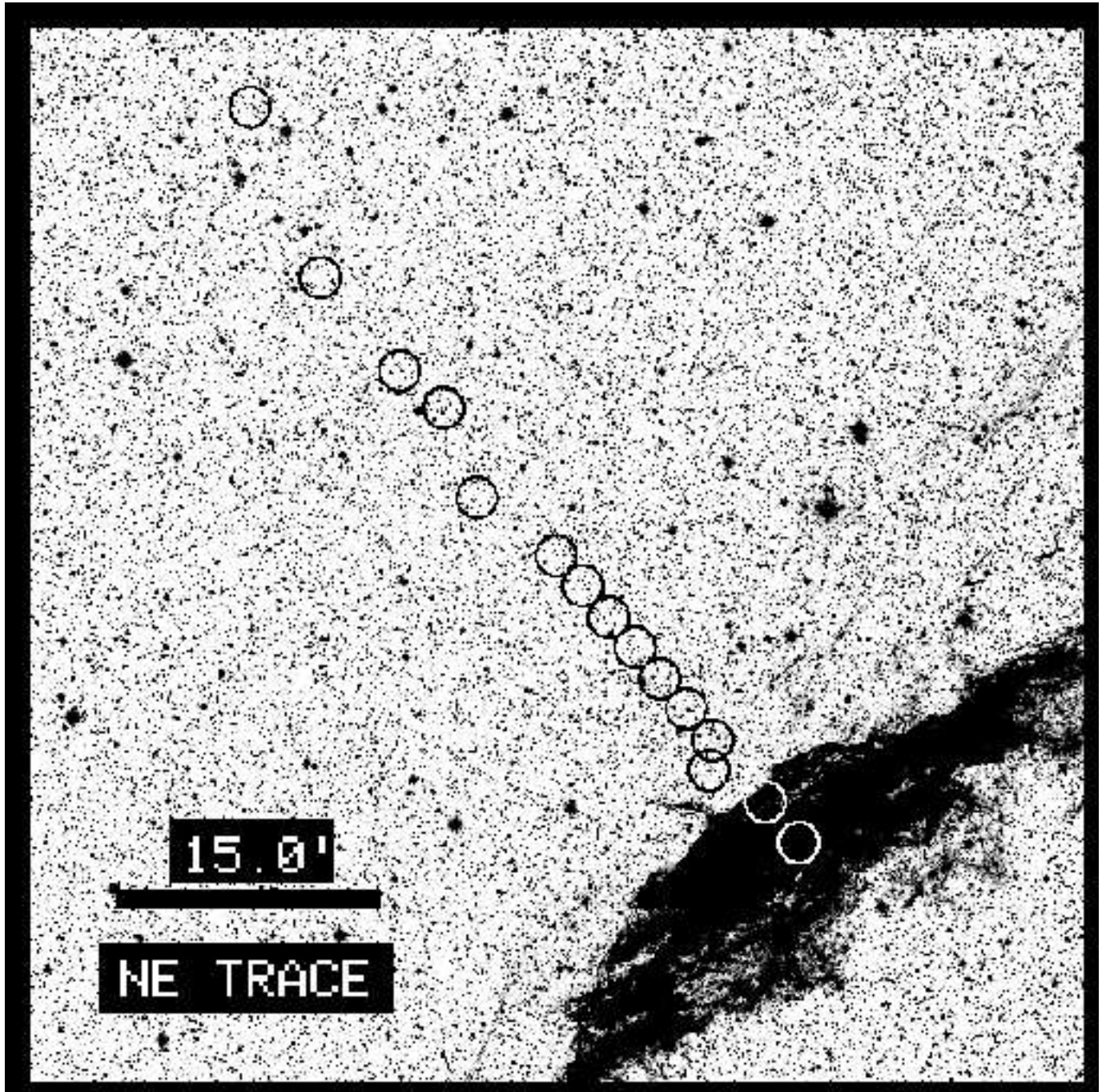


Figure 3a.

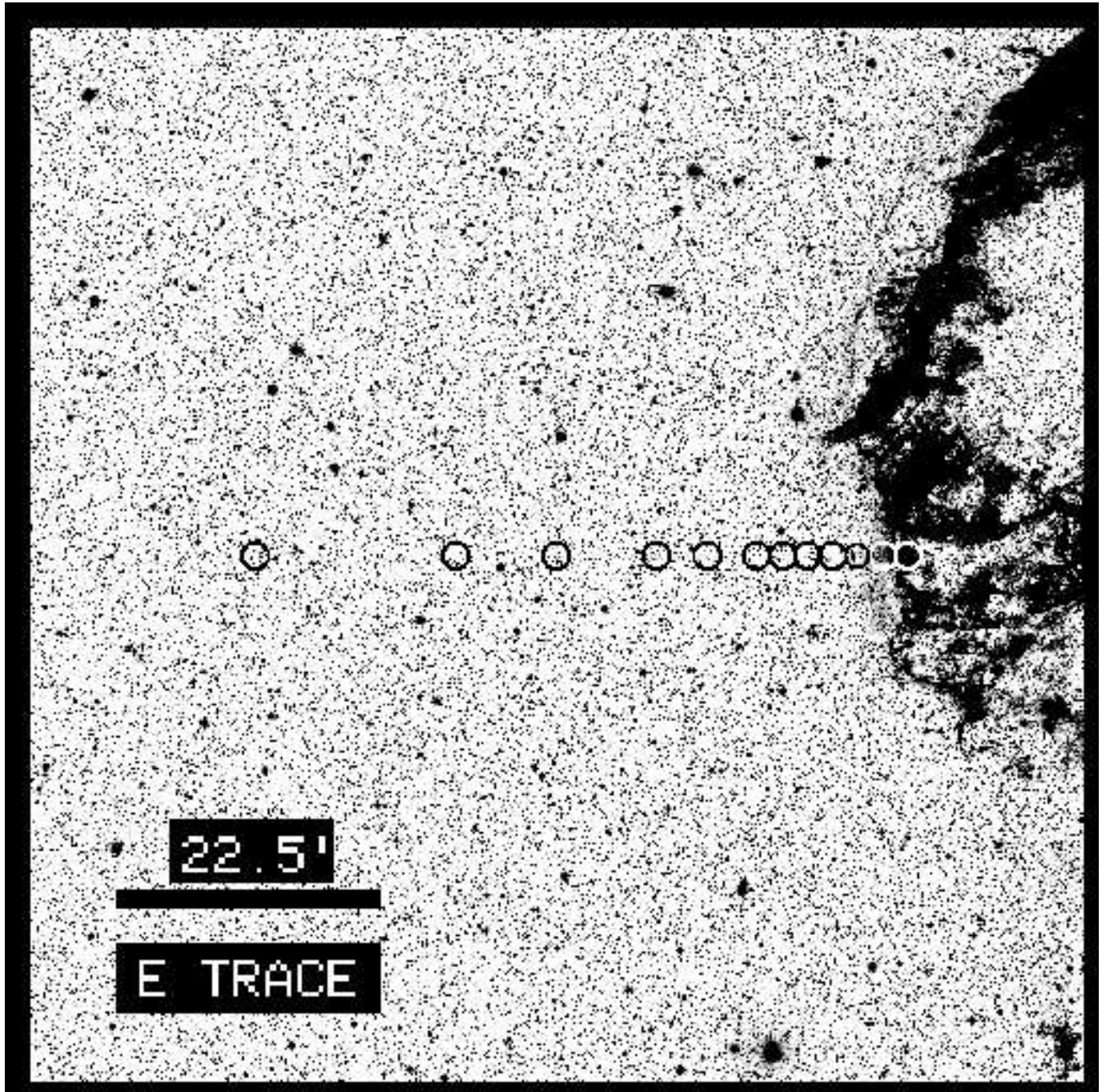


Figure 3b.

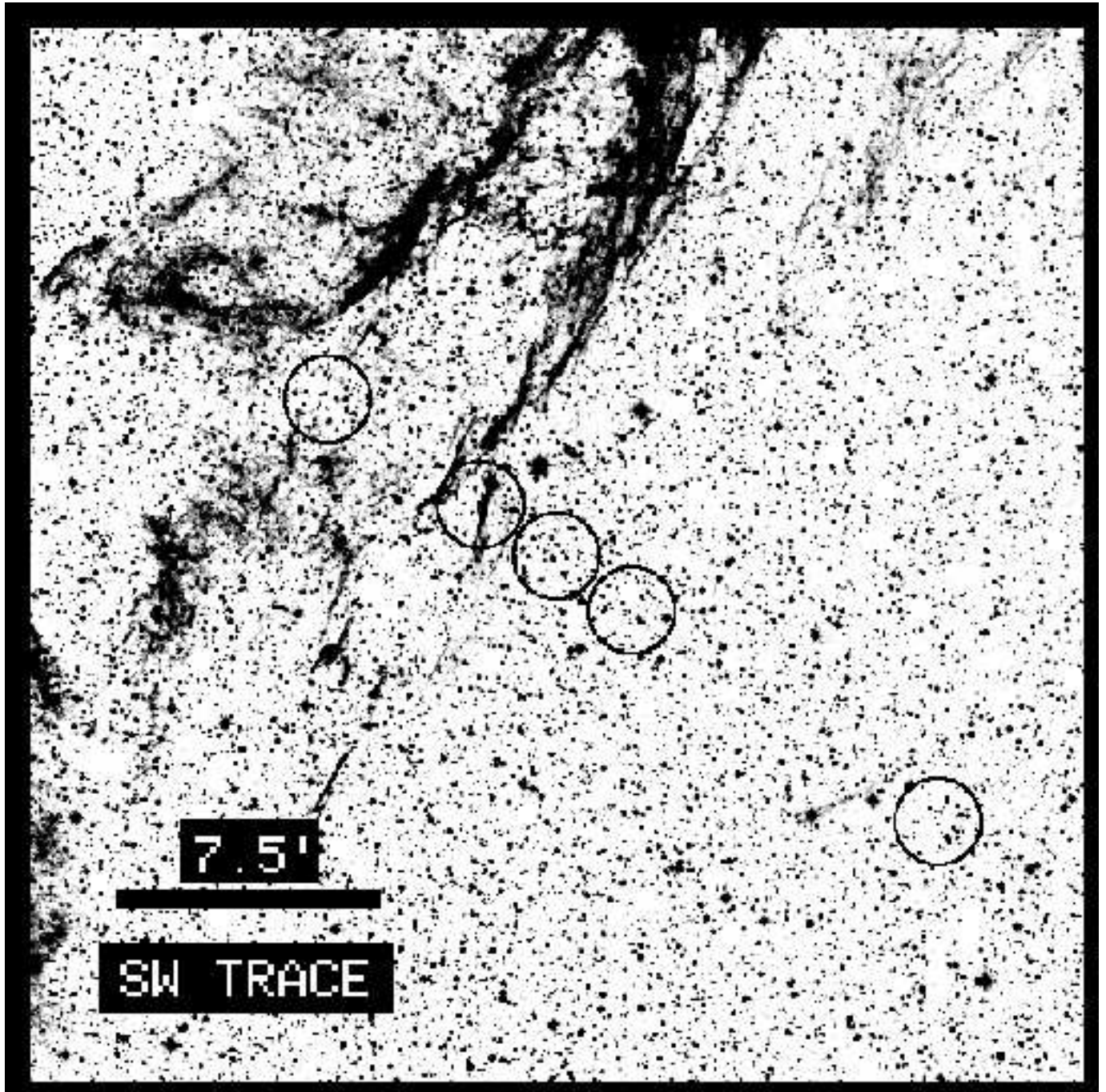
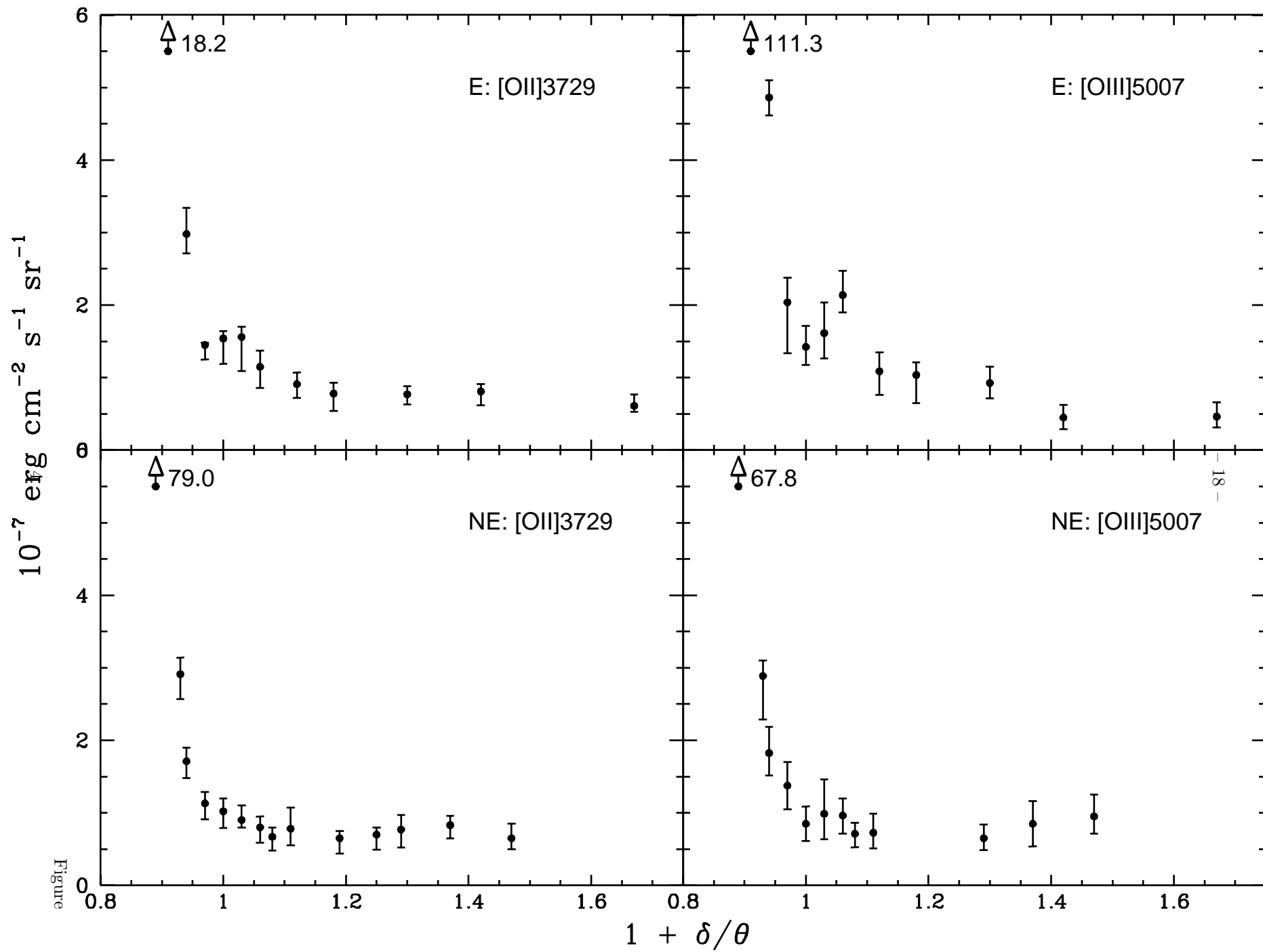


Figure 3c.



Figure

18